Molecular BioSystems

Accepted Manuscript

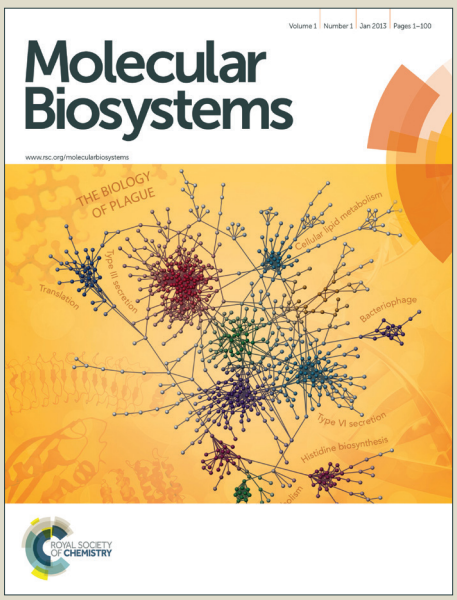

ROYAL SOCIETY OF CHEMISTRY

www.rsc.org/molecularbiosystems

Recent Advances in the Structure-based Rational Design of TNKSIs

Peng Zhan[1,2*], *Yu'ning Song*[1], *Yukihiro Itoh*[2], *Takayoshi Suzuki*[2,*], *Xinyong Liu*[1,*]

[1]Department of Medicinal Chemistry, Key laboratory of Chemical Biology (Ministry of Education), School of Pharmaceutical Sciences, Shandong University, 44, West Culture Road, 250012, Jinan, Shandong, P. R. China

[2]Graduate School of Medical Science, Kyoto Prefectural University of Medicine, 1-5 Shimogamohangi-Cho, Sakyo-Ku, Kyoto, 606-0823, Japan

Abstract: Human tankyrases 1 and 2 (TNKS1/2) are attractive pharmacological biotargets, especially for the treatment of specific cancer. This article provided a fairly comprehensive overview of structural biology of TNKS/inhibitor complex and current medicinal chemistry strategies being used in the structure-based rational design of tankyrase-specific inhibitors.

Keywords: Tankyrases, Inhibitor, Rational drug design, Scaffold-hopping, Medicinal chemistry strategies.

1. Introduction

The poly(ADP-ribose) polymerase (PARP) protein superfamily has multifacet functions in cellular processes including DNA repair and Wnt signalling. Most of the efforts to pharmacologically target PARPs have already focused on the most abundant PARP1 and PARP2, it is noteworthy that recent investigations highlighting the function of additional family members, tankyrase 1 (TNKS1) and tankyrase 2 (TNKS2), in the control of Wnt signalling (as the regulators of Axin ubiquitylation and degradation) has fuelled great interest in the exploitation of novel inhibitors towards these PARP members [1]. TNKS1/2 are different from other enzymes of the PARP family by the structural characteristics in the catalytic site, the presence of an ankyrin repeat protein-interaction domain and a sterile α-motif multimerization domain. TNKSs can utilize NAD^+ as a substrate to produce ADP-ribose polymers onto acceptor proteins (namely PARsylation) [2]. As shown in **Figure 1**, the catalytic

*Corresponding authors. E-mail addresses: zhanpeng1982@sdu.edu.cn (Zhan, P.); suzukit@koto.kpu-m.ac.jp (Suzuki, T.); xinyongl@sdu.edu.cn (Liu, X.Y.).

domain of TNKSs splits NAD^+ into nicotinamide (**I**) and ADP-ribose (**II**), which is covalently linked to a growing ADP-ribose polymer or to a target protein [2]. From the perspective of drug design, the key H-bond interactions with the nicotinamide group benefit the defination the basic pharmacophore elements of TNKSs inhibitors (TNKSIs) binding to the nicotinamide subsite [2].

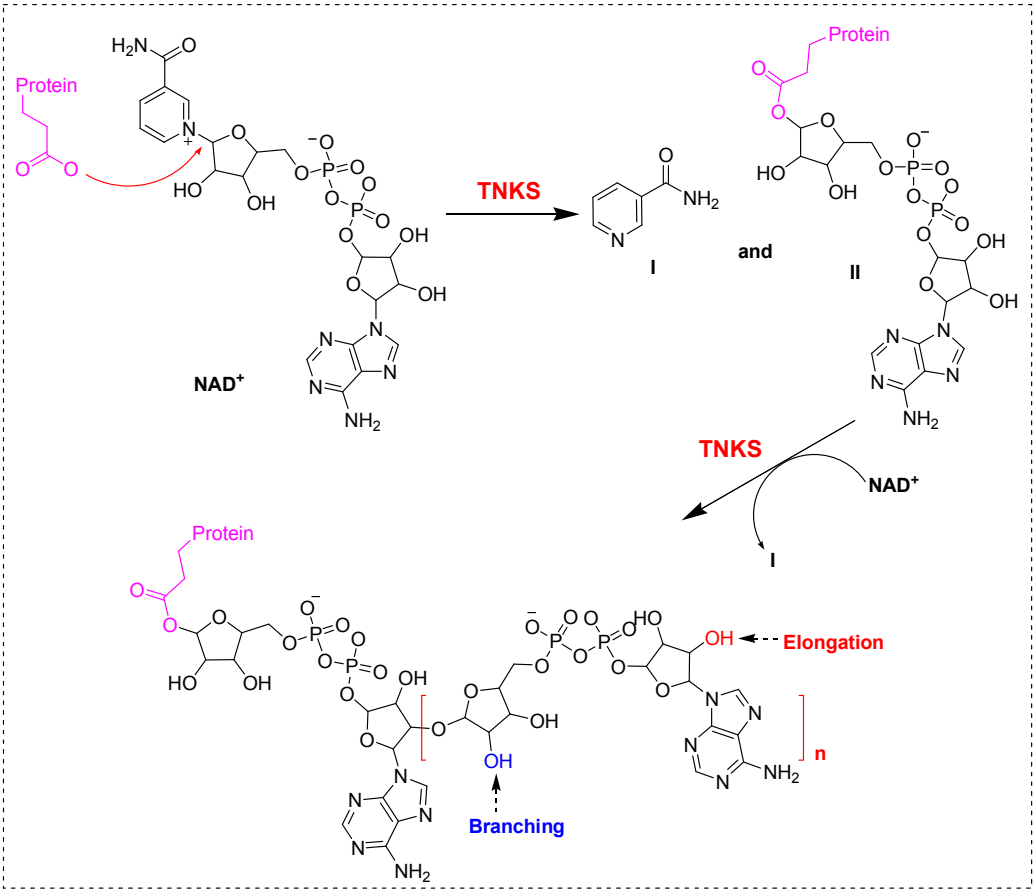

Figure 1. Post translational modification reaction (ADP-ribosylation) catalyzed by TNKSs. The ADP-ribose moiety from NAD^+ is transferred to a glutamic acid residue of the acceptor protein to provide **II**, releasing nicotinamide (**I**).

TNKSs are implicated in various processes, including cell proliferation, telomere homeostasis, mitotic spindle formation, vesicle transport linked to glucose metabolism, lung fibrogenesis and myelination, as well as viral replication, suggesting that TNKSs are promising biotargets with extensive clinical utilities, especially for the treatment of specific cancers [1,3,4]. Within the last few years, small-molecule TNKSIs have proved to be valuable pharmacological tools to investigate the

therapeutic benefits of targeting these proteins and as potential lead compounds [4]. A large amount of X-ray structural data have also been accumulated in the last years for adducts of TNKSs with the main classes of inhibitors. Hitherto, the thorough reviews of TNKSIs as well as their pharmacological implications have been reported elsewhere [1,2,4,5]. However, no comprehensive survey has been published to outline the structural biology implications and the medicinal chemistry strategies employed in the discovery of bioactive TNKSIs, which is the aim of this minireview. As the Chinese proverb said, "teaching one to fish is better than giving him fish". We hope this review will provide useful methodologies to medicinal chemists who are interested, and introduce some inspirations for newcomers in this field, by telling them what has been achieved, where we are and what will be next.

2. Serendipitously discovered chemotypes of TNKSIs

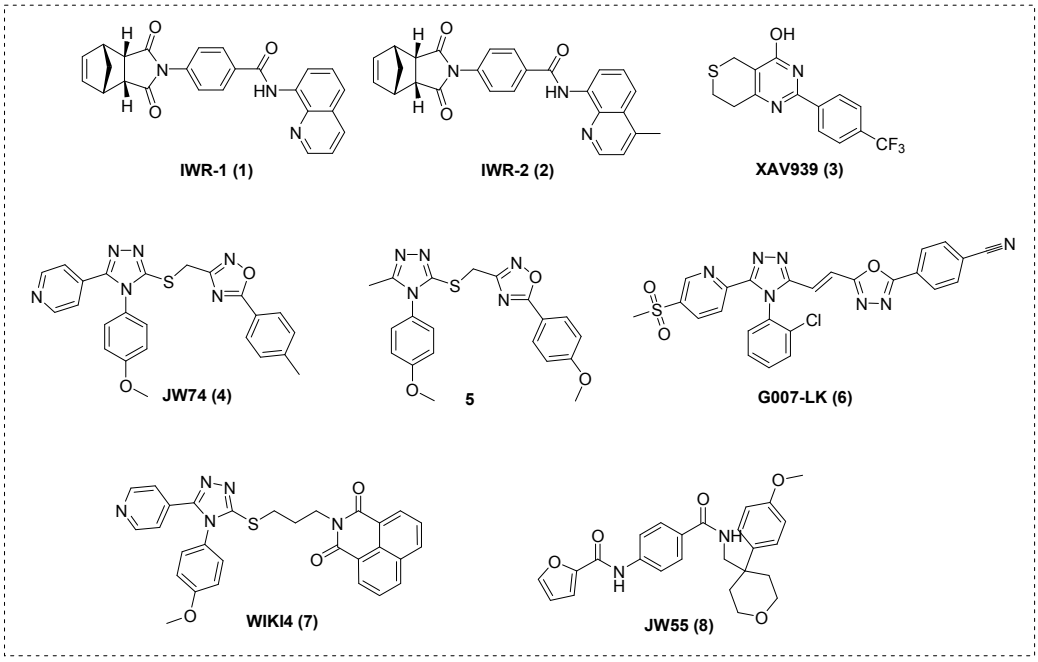

Figure 2. Structures of specific TNKSIs from early cellular phenotypic and biochemical HTS.

Up to now, a lot of structurally diverse TNKSIs have been identified by cell-based high-throughput screening (HTS) campaign or serendipitous discovery (**Figure 2**). In 2009, several structurally distinct chemotypes, namely, IWR1 (**1**), IWR2 (**2**) (IWR: inhibitor of Wnt-Response) [6], and XAV939 (**3**) [7], were identified as active and selective small molecule TNKSIs by HTS of diverse synthetic chemical library

targeting Wnt signaling (**Figure 2**). Originally, they were identified as novel inhibitors of Wnt/β-catenin signaling. Furthermore, it was demonstrated that they mediated their inhibition on Wnt/β-catenin signaling by targeting the enzymatic activities of TNKS1/2. For instance, IWR2 inhibited TNKS1/2 with IC_{50} values of 160 nM and 350 nM, respectively [6]. XAV939 was originally demonstrated to be a moderate PARP1/2 inhibitor wirh IC_{50} values of 2.2 μM and 0.11 μM, respectively, then was further identified as a more active TNKS1/2 inhibitor (IC_{50} = 11 nM, 4 nM)[7]. At present, these compounds have been employed as biological tools to probe the Wnt pathway and the biological functions of TNKSs in cancer and other cellular functions [8-10].

Besides, a 1,2,4-triazole derivative JW74 (**4**) was identified as an inhibitor against Wnt signaling in a HEK293-STF assay and demonstrated active and selective inhibition of the TNKS1/2 (IC_{50} = 2.55 μ M, 0.65 μ M, respectively, in HEK293-STF cells) [11]. Further, long-term treatment with JW74 (**4**) suppressed the growth of tumor cells in ApcMin mice (multiple intestinal neoplasia) and human colorectal cancer in a mouse xenograft model. It also affected cell cycle progression and induced apoptosis and differentiation in osteosarcoma cell lines [11]. These findings rationalized further (pre)clinical investigation of this novel molecule as additional modality for TNKS-targeted therapeutics [11]. Further optimization through synthesis and screening of a focused molecule collection of this initial hit resulted in the discovery of compound **5** with an IC_{50} value of 33 nM for TNKS2 and > 19 μM against PARP1/2 [12]. By introducing a methyl group to replace the pyridyl group of **4**, diminished activity against P450 isozyme was observed. In consequence, chemical analoging evolution of **4** provided G007-LK (**6**), as a highly potent and selective TNKS1/2 inhibitor (IC_{50} values of 46 nM and 25 nM, respectively; cellular EC_{50}: 50 nM), with remarkable pharmacokinetic profiles in mice, combined with metabolic stability and druggability [13]. Most worthy of mention is that G007-LK could also suppress APC mutation-driven colorectal tumor growth [14].

In a similar manner, WIKI4 (**7**) [15,16] and JW55 (**8**) [17] were also identified as highly bioactive and specific TNKSIs using HTS campaign targeting Wnt/β-catenin signaling.

Collectively, these findings provided novel chemotype leads for discovery of pharmaceutically useful drug candidates targeting canonical Wnt/β-catenin signaling through inhibiting TNKS1/2, for treatment of cancer and other diseases.

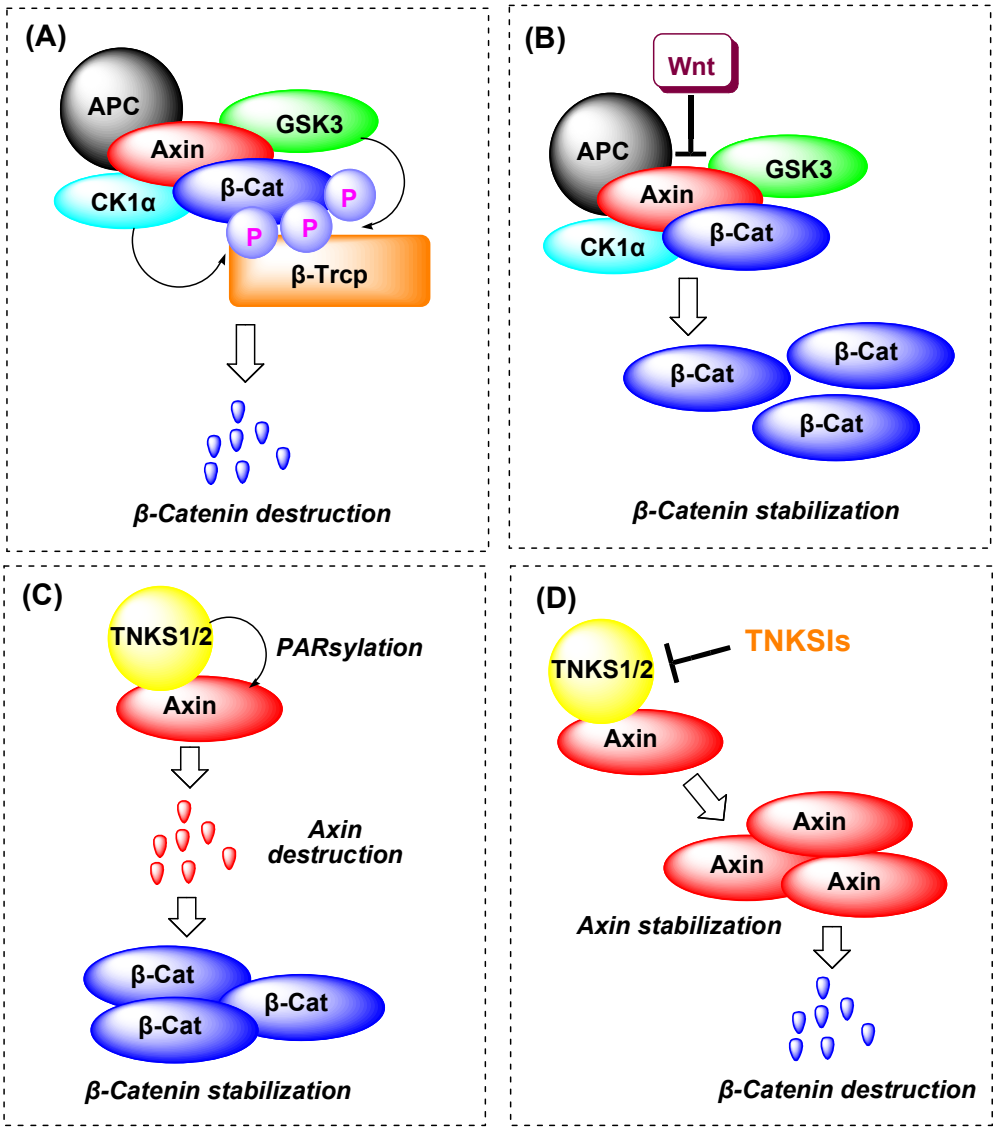

Figure 3. The action of mechanism of TNKSs and TNKSIs in Wnt/β-catenin signaling pathway.

During the course of lead discovery, the action of mechanism of TNKSIs in Wnt/β-catenin signaling pathway has been gradually elucidated. As shown in **Figure 3A**, β-catenin (β-cat) was phosphorylated by the β-catenin destruction complex

containing axin (the rate-limiting protein of the destruction complex), CKIa, GSK3 and APC. Phosphorylated β-catenin was recognized by an ubiquitin ligase β-Trcp, and degraded through the ubiquitination/proteasome pathway; Wnt stimulation inhibited β-catenin phosphorylation/destruction, providing increased β-catenin protein (which then enters the nucleus to activate transcription) (**Figure 3B**); TNKS1/2 can interact with a highly conserved domain of axin and promote the destruction of axin, likely through axin poly(ADP-ribosyl)ation (PARsylation) to stimulate its degradation. As such, β-catenin stabilization was observed, which resulted in the accumulation and nuclear translocation of β-catenin, and activation of the transcription of target genes (**Figure 3C**). As shown in **Figure 3D**, when the catalytic function of TNKSs was inhibited by specific TNKSIs, then the PARsylation-dependent axin degradation was prevented, leading to β-catenin destabilization and inhibition of Wnt signaling.

2. Structural biology of TNKS/TNKSI complex

The reported high-resolution co-crystal structures of TNKS1/2 complexed with TNKSIs reveal that the potency and selectivity of these small-molecule TNKSIs can be rationalized by how they fit within the nicotinamide pocket (NAD^+-binding site of the catalytic domain) or a distinct adenosine subsite. For instance, XAV939 (**3**) could bind with the nicotinamide pocket *via* similar interactions as seen for other PARP-inhibitor complexes, with three conserved H-bonds between the binding pocket and the ligand, through the lactam carbonyl and NH group in the quinazolinone group (namely, the carbonyl O serves as hydrogen acceptor with OH of Ser1068/Ser1221 and with NH of Gly1032/Gly1185, the NH serves as hydrogen donor with C=O of Gly1032/Gly1185) [18,19]. Additional π-stacking interactions were formed between the lactam and Tyr1071/Tyr1224, the CF_3-phenyl points to a hydrophobic subpocket. The binding modes of XAV939 (**3**) in the crystal of TNKS2/1 were shown in **Figure 4** and **Figure 5**, respectively.

The co-crystal structures of TNKS1/IWR2 (**Figure 6**) and TNKS2/IWR1 (**Figure 7**) revealed an alternative binding mode for PARP family proteins that IWRs did not form contacts with the nicotinamide binding groove, but bound to an induced pocket (formed only upon binding the inhibitor), highlighting a new space in the chemical

variability of TNKSIs. There were two pivotal H-bonds between IWR2/1 and TNKS1/2: one between a C=O of the pyrrolidine dione moiety and the backbone NH of Tyr1213 or Tyr1060, another one between the C=O of the amide and the backbone NH of Asp1198 or Asp1045. Besides, the CH at the 6-position of the quinoline engaged in one H-bond with the backbone C=O of Gly1196 (TNKS1) [20,21].

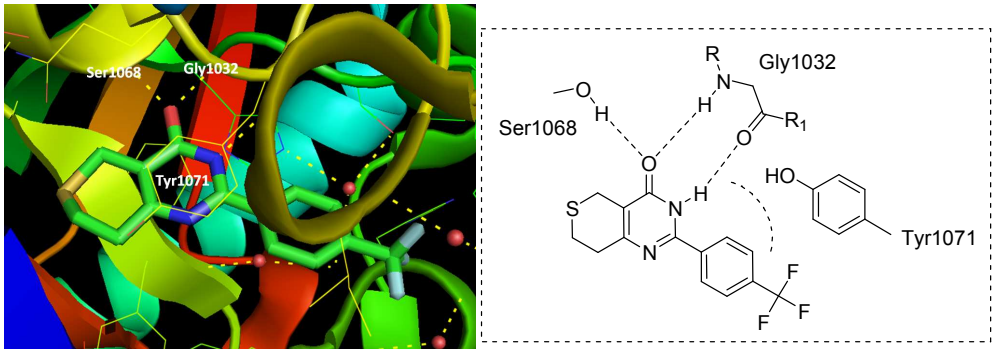

Figure 4. Human TNKS2-catalytic PARP domain in complex with XAV939 (**3**) (carbon: colored in green) (PDB code: 3KR8, resolution: 2.10 Å). Key H-bond interactions were shown as yellow dashed lines [18].

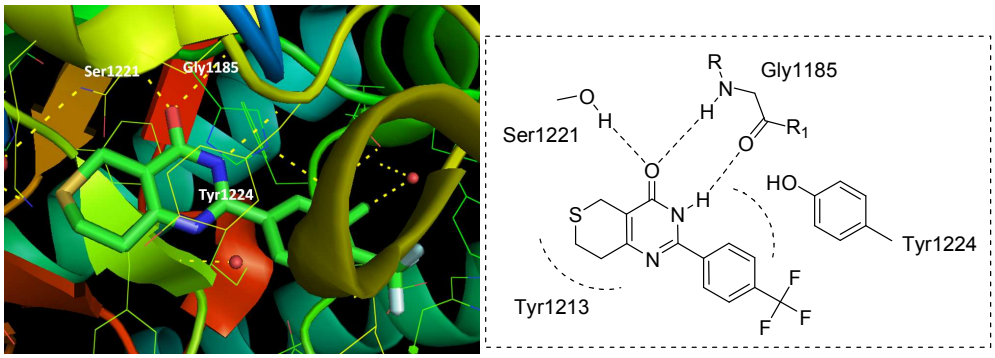

Figure 5. TNKS1 complexed with XAV939 (**3**) (carbon: colored in green) (PDB code: 3UH4, resolution: 2.00Å) [19].

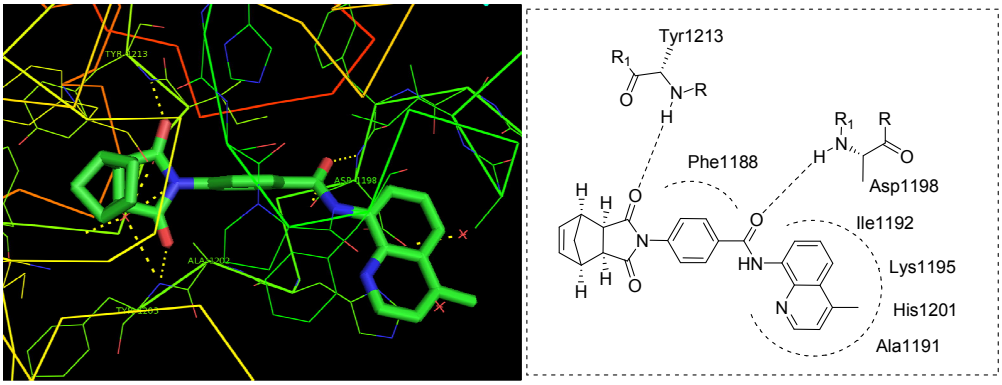

Figure 6. Crystal structure of TNKS1 with IWR2 (carbon: colored in green) (PDB code: 4DVI. Resolution: 1.90Å) [20]. IWR2 binds to an induced pocket other than the nicotinamide pocket.

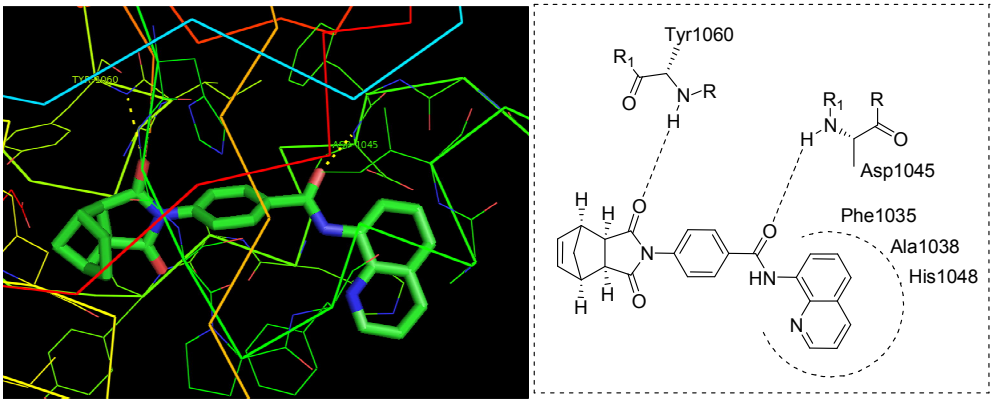

Figure 7. Crystal structure of human TNKS2 in complex with IWR1 (carbon: colored in green) (PDB code: 3UA9, resolution: 2.15Å) [21].

The co-crystal structures of 1,2,4-triazole **5**, G007-LK (**6**) and WIKI4 (**7**) complexed with catalytic domains of TNKS1/2 demonstrated that these inhibitors bound to the induced pocket, which were similar to IWR1/2 (**Figures 8-10**) [12,13,16].

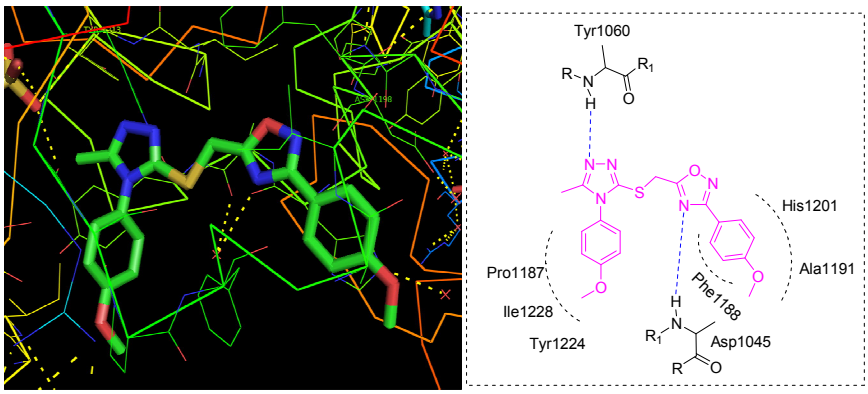

Figure 8. The co-crystal structure of compound **5** complexed to TNKS1 (PDB code: 3UDD, carbon: colored in green).

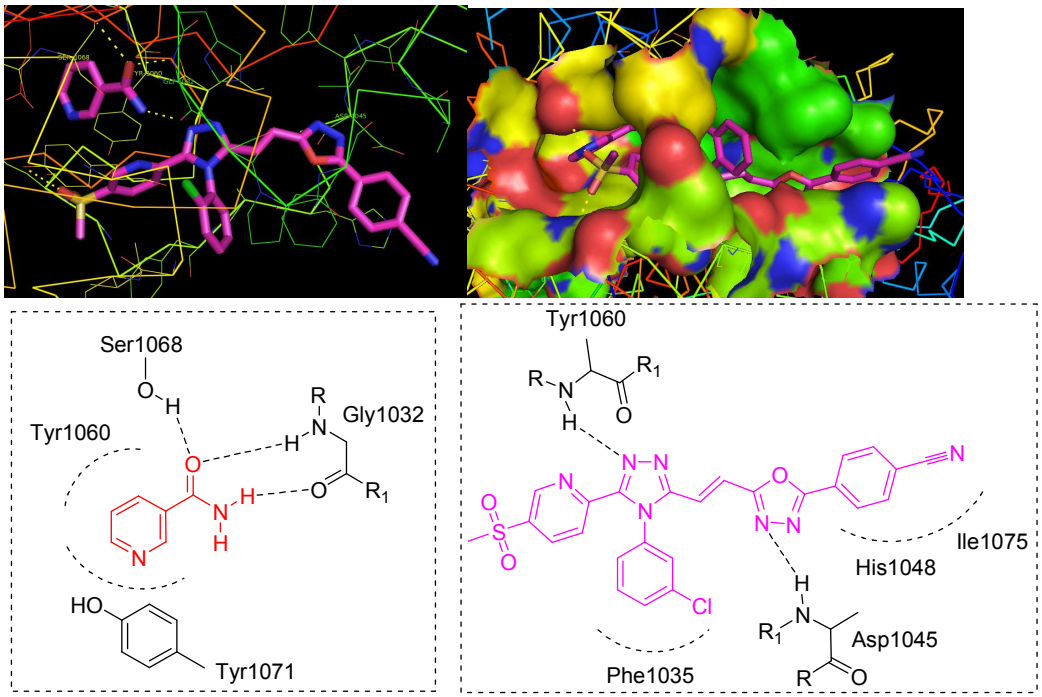

Figure 9. Crystal structure of TNKS1 in complex with G007-LK (**6**) and nicotinamide (PDB code: 4HYF, resolution: 2.80Å).

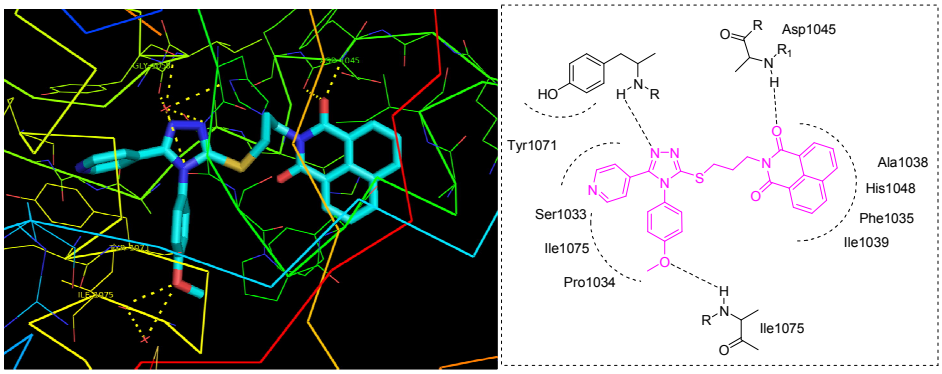

Figure 10. Crystal structure of TNKS2 in complex with WIKI4 (**7**). (PDB code: 4BFP, resolution: 2.40Å) [16].

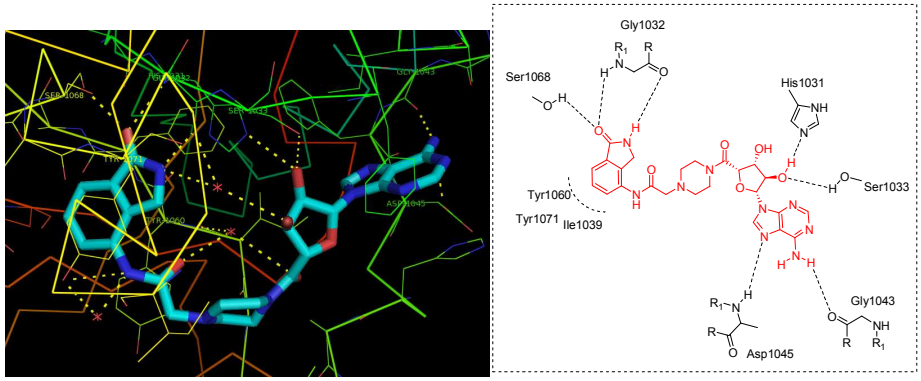

Figure 11. Crystal structure of TNKS2 in complex with EB-47 (**9**). (PDB code: 4BJ9, resolution: 2.05Å).

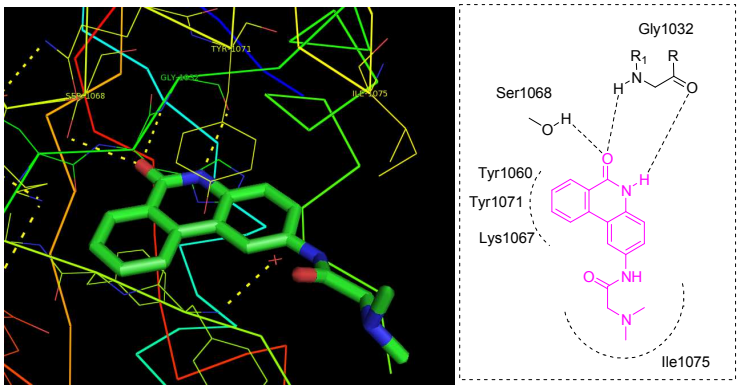

Figure 12. Crystal structure of TNKS2 in complex with PJ-34 (**10**) (PDB code: 4BJB, resolution: 2.30 Å).

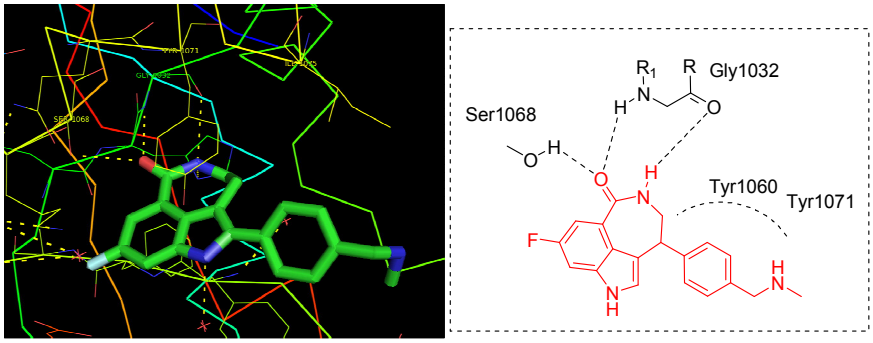

Figure 13. Crystal structure of TNKS2 in complex with rucaparib (**11**) (PDB code: 4BJC, resolution: 2.20Å).

Furthermore, the binding modes of several existing PARP inhibitors with TNKS2 were also determined by X-ray crystallography, including EB-47 (**9**), PJ-34 (**10**) and rucaparib (**11**, a clinical ARTD1 inhibitor candidate) (**Figures 11-13**). Rucaparib displayed IC_{50}s of 24 and 14 nM for TNKS1/2, respectively. It was revealed flexibility of the binding site with implications for further drug design against TNKSs and other PARPs. The binding modes of PJ-34 (**10**) and rucaparib (**11**) in the nicotinamide binding site were similar to that of XAV939 (**3**). EB-47 could mimic the substrate NAD^+ and extended from the nicotinamide to the adenosine subpocket [22]. Collectively, these complexes of TNKSs/TNKSIs provided critical insights into the molecular basis of the high affinity and gave valuable clues for the next round of structure-based drug-design campaign for high-affinity subtype-selective TNKSIs.

3. Medicinal chemistry strategies employed in the discovery of TNKSIs

Over the past few years, many emerging medicinal chemistry strategies have been employed in scaffold hopping and structure-based lead discovery of TNKSIs. Undoubtedly, only using the above described structural biology information as a staring point, would the application of these classical or latest strategies in the discovery of biologically active TNKSIs be highly productive. In the following section, we will present the discussions of the case-studies for seeking TNKSIs by various structure-based approaches, such as dual binders, structure-efficiency relationship (SER)-guided modification, crystallographic overlays-based molecular hybridization, structure- and biophysics-driven fragment-based ligand design (FBLD), and orthodox bioisosteric replacement.

3.1 Dual binders (Bidentate inhibition) targeting both the nicotinamide pocket and the induced pocket

Multi(dual)site inhibitors could bind simultaneously in more than one regions in a target by combining several structural elements necessary for recognition by target protein into a single ligand, thus allowing to maximize contacts with its complementary binding pocket. These molecules, if properly designed, would possess significantly improved affinity and high selectivity when compared with single-site compounds, owing to lower entropic penalty for simultaneously binding with multiple sites [23]. As described above, besides the nicotinamide pocket, some novel TNKSIs have recently been characterized to bind to an induced pocket. Consequently, a bidentate-binding (dual binders) strategy that simultaneously utilized the the nicotinamide pocket and the induced pocket has been applied to rational design of TNKSIs.

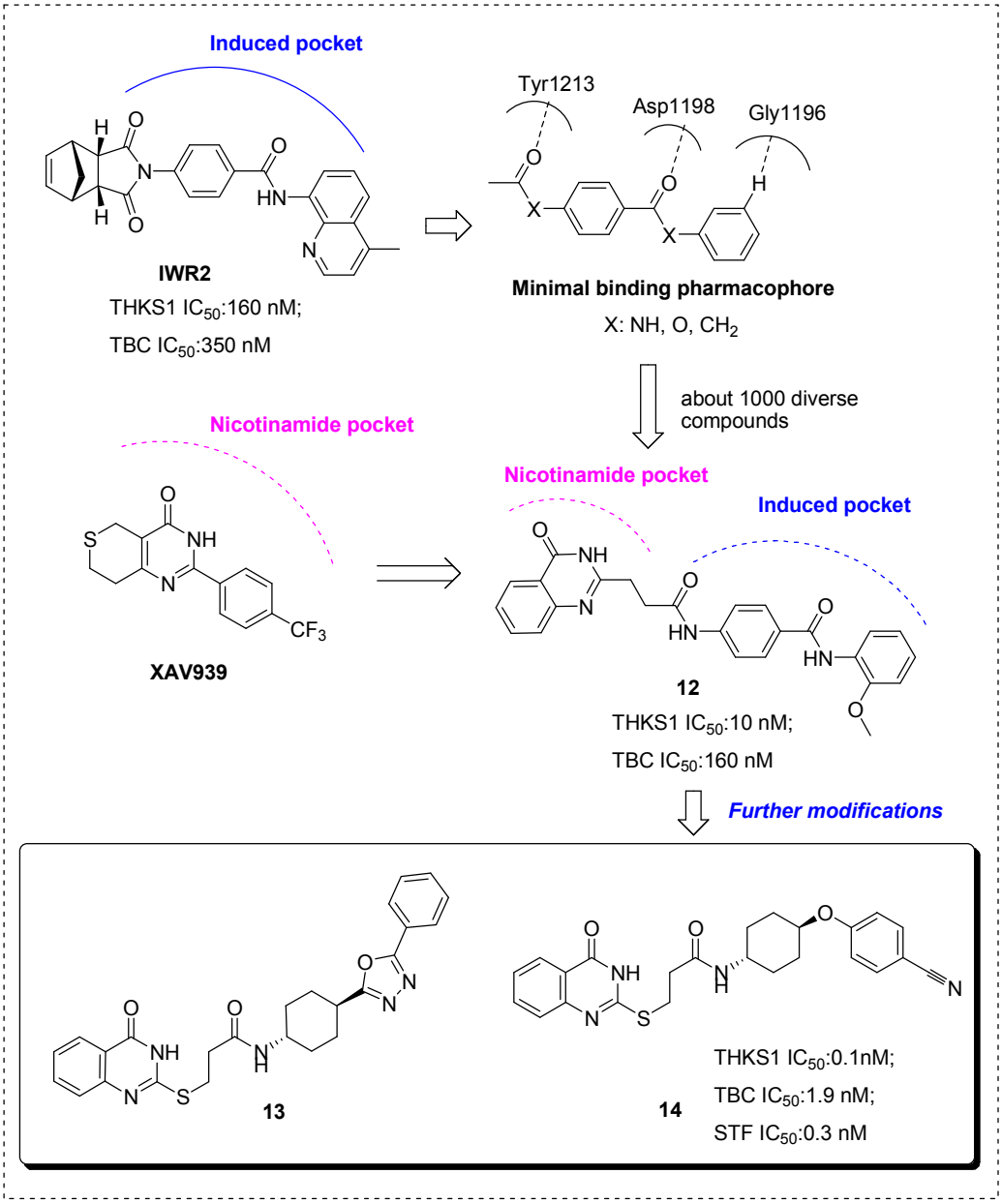

Figure 14. Identification of dual binders **12-14** targeting both the nicotinamide pocket and the induced pocket via substructure search and screening, and further optimization.

As shown in **Figure 14**, hit compound **12** was identified as a novel efficient and selective TNKS "dual-binder" that binds to both the nicotinamide pocket and the induced pocket *via* a combination of pharmacophore model-guided substructure searching of compound library and HTC [24].

Table 1. Inhibitory activity in TNKS1/2 and PARP2 biochemical assays.

	IC_{50} (uM)			
	TNKS1	**TNKS2**	**PARP2**	**Wnt Pathway**

IWR1	0.151	0.038	>25	136
IWR2	0.192	0.036	n.d.	163
XAV939	0.068	0.017	n.d.	272
12	0.008	0.002	0.931	36

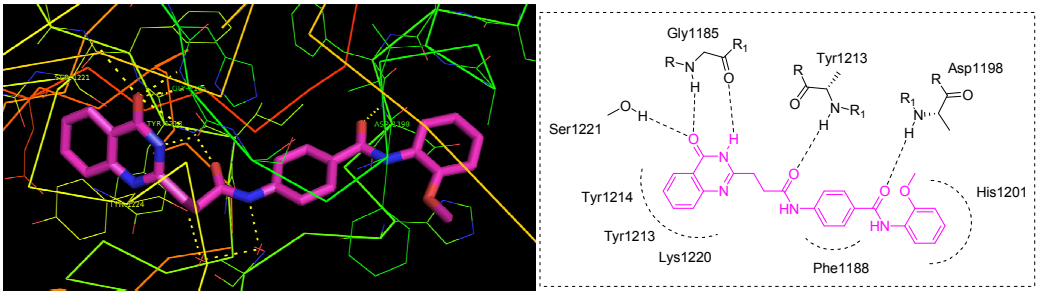

Figure 15. Crystal structure of TNKS1 with **12** (PDB code: 4I9I, resolution: 2.40Å).

Compound **12** could bind to the nicotinamide pocket *via* three H-bonds and to the induced pocket *via* two key H-bonds (**Figure 15**). The hydrophobic contacts between **12** and TNKS1 (such as Phe1188 and His1201) were also observed. The crystal structure of TNKS1/**12** complex afforded reasonable explanation for their specific interactions and gave insights for the further exploitation of "dual-binders" as potent and selective TNKSIs [24]. Then the structure- and property-based refining of compound **12** resulted in the discovery of more active and selective TNKSIs (**13**,**14**) with optimized pharmacokinetic profiles, which were well suited to in-depth investigations *in vivo* as tool molecules [25].

3.2 Structure-Efficiency Relationship (SER)-guided Modification

The usage of efficiency indices has already become one of the most effective approaches to more rapidly discovery and improve quality of chemical entities [26,27]. The ligand efficiency (LE) and lipophilic efficiency (LipE = pIC_{50} - log D) were the most two commonly used parameters to rationalize hits with high quality and highly optimized molecules, respectively [28]. Generally speaking, LE should be adopted as decision-making parameter during early hit identification stage to maximize potency versus molecular size, whereas LipE should be adopted during later optimization phase to balance potency and lipophilicity [28].

XAV939 was considered to be an attractive starting point for further modification for it′s prominent advantages including low nanomolar enzymic inhibition, 78 nM

potency at the cellular level, high LE value (0.55), and good lipophilic efficiency (LipE = 4.2 based on measured log D of 4.1). Even so, the selectivity of **XAV939** versus other PARP family members (10-100 fold) has yet to be improved, the microsomal stability (rat liver microsomal extraction ration, rLMER = 0.88), and solubility (10 μM at pH 1, < 5 μM at pH 6.8) was lower, which was not well suited for further in vivo validation studies.

In order to prove the impact of TNKS inhibition in preclinical models, a potent and selective TNKS inhibitor *in vivo* was required. Thus, the highest priority for back-up series was to improve activity, selectivity, metabolic stability, and solubility. As **XAV939** had a measured logD of 4.1, it was hypothesized that the poor properties and off-target liabilities may well be improved by reducing the lipophilicity. Therefore, beginning with **XAV939**, LipE score was explored to further probe the chemical structural space of TNKS and the optimum compatibility for inhibitors.

As shown in **Figure 16**, by utilizing a combination of structure-based design and structure-efficiency relationships (SER) to drive the optimization based on LipE rather than absolute potency, XAV939 (cellular IC_{50} = 78 nM) was successively evolved to a more stable, more efficient but less potent dihydropyran motif **15** (cellular IC_{50} of 2.7 μM), compound **16** (cellular IC_{50} of 1.9 μM) before finally optimizing to NVP-TNKS656 (**17**) (cellular IC_{50} of 3.5 nM) as an orally active inhibitor of Wnt activity in the MMTV-Wnt1 mouse xenograft model, which is well suited for the next step of in vivo validation studies [29].

The thermodynamic profiles of key compounds identified during the optimization showed that a LipE-driven optimization approach generated molecules with enthalpy-driven binding. Thus, the use of LipE driven decision making facilitated this rapid scaffold decoration and potency improvement without overly relying on lipophilic interactions and the identification of any other off-target effects.

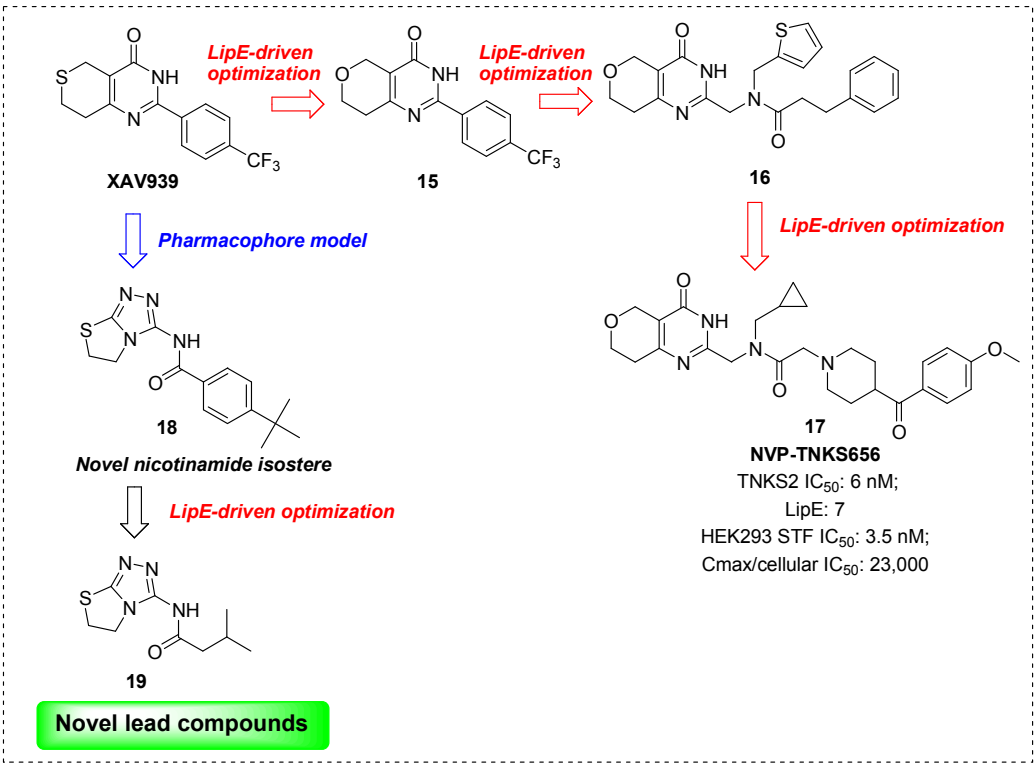

Figure 16. Discovery of novel TNKSIs *via* a combination of structure based design and structure efficiency relationships.

Guided by the pharmacophore model, [1,2,4]triazol-3-ylamine **18** was identified as a highly potent TNKSI that represents an additional isostere of nicotinamide-based PARP inhibitors with significant selectivity *versus* the other members in PARP family. Through the utilization of LipE based SER driven optimization, a novel series of extremely efficient and selective TNKSIs (such as **19**) with highly favorable properties was created. The application of structure-based pharmacophore model, drug-like properties and lipophilic-efficiency-focused drug design was proven highly effective and successful (**Figure 16**,**17**). Therefore, in the case of TNKS, LipE was a usefully predictive tool for the rapid discovery of efficient and selective molecules *in vivo* [30].

Table 2. Bioactivities and efficiency indices of XAV939 and its [1,2,4]triazol-3-ylamine isostere.

Compds	TNKS2		IC_{50} (μM)				clogP
	LipE	LE	TNKS2	PARP1	PARP2	STF[a]	
XAV939	5.9	0.55	0.0053	1.37	0.106	0.078	2.3
18	4.3	0.50	0.031	nd	>19	2.39	3.1
19	5.7	0.66	0.103	55.3	nd	6.46	1.3

[a]HEK293 SuperTopFlash reporter gene assay.

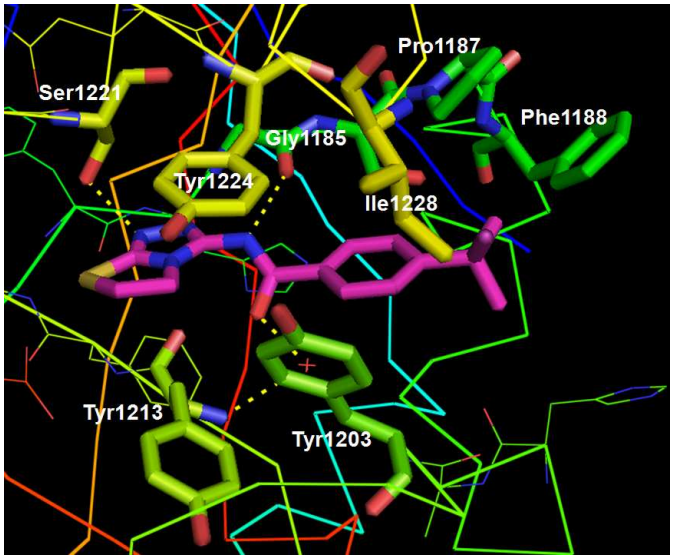

Figure 17. Co-crystal structure of **18** in TNKS1 (PDB code: 4KRS, resolution: 2.29Å). H-bonds are shown as yellow dashed lines.

3.3 Molecular hybridization based on crystallographic overlays

Molecular hybridization is a classical concept in structural modifications based on the combination of basic pharmacophore elements of diverse bioactive molecules to generate a novel hybrid entity with improved activity and favorable properties, when compared to the prototypes [31]. Crystallographic overlays-based molecular hybridization (namely, knowledge-based pharmacophore hybridization) [32] requires knowing beforehand of structural biology information about the biotarget of interest, which represents a rational approach of molecular hybridization compared to the other ligand-based methodologies. In the following two instances, using crystallographic overlays of the known TNKSIs/TNKS complex as a starting point, and structure-based molecular hybridization, a novel set of potent and selective TNKSs with improved pharmacokinetic properties were created.

Compound **20** was a previously described TNKSI with moderate potency (TNKS1, IC_{50} = 0.20 μM) that suffered from poor pharmacokinetic properties (the amide is prone to hydrolysis in both rat and mouse plasma). It was discovered that oxazolidinone **20** bound to the induced pocket of TNKS1 in a similar manner to that of IWR1/2 (**Figure 18**). The crucial interactions were composed of three H-bonds: the

C=O of the amide with Asp1198; the C=O of the oxazolidinone with Tyr1213; one C=O…H-C-typed H-bond between the C-H in the C-6 of the quinoline and the backbone C=O of Gly1196 (TNKS1). Besides, the quinoline ring involved in a π-stacking contact with His1201. Overlay of the TNKS/TNKSI co-crystal structures of HTS hit **21** (TNKS1, IC_{50} = 0.024 μM) and **20** (**Figure 18**) demonstrated that the C=O groups of the benzimidazolone and amide moieties engaged in H-bond interactions with Asp1198. Moreover, the electron-deficient quinoline group of **20** overlaid well with the benzimidazolone phenyl group of **21**, and was associated with a favorable stacking interaction with His1201. These specific noncovalent interactions provided valuable implications for rational drug design. Combination of the oxazolidinone moiety of **20** with the cyclohexyl benzimidazolone of **21** created **22** and **23** (*via* further modification) with improved potency (TNKS1, IC_{50} = 4 nM, 1 nM, respectively) and orally bioavailable pharmacokinetic properties (**Figure 19**) [33].

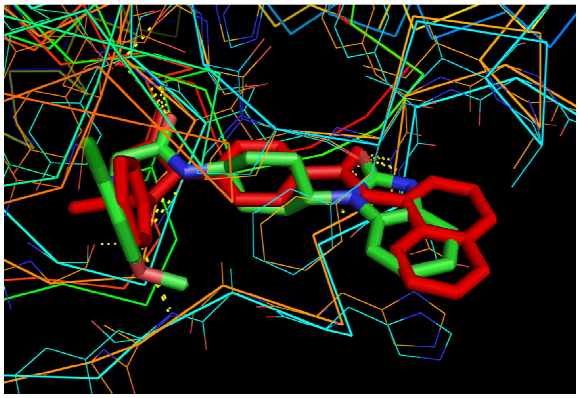

Figure 18. Overlay of the TNKS1 co-crystal structure of **20** (red) (PDB code: 4K4F, resolution: 2.90Å) and **21** (green) (PDB code: 4K4E, resolution: 2.30Å) [33].

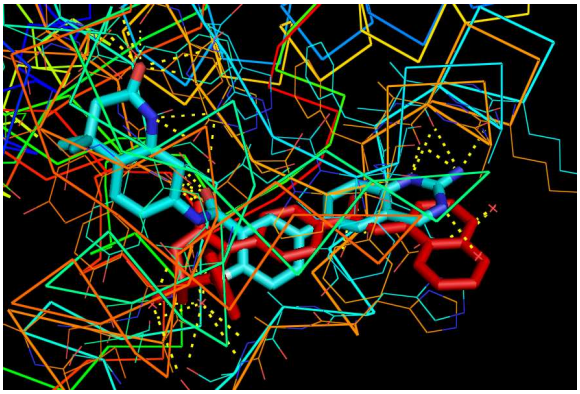

Figure 19. Overlay of the TNKS1 co-crystal structure of **20** (red) (PDB code: 4K4F, resolution: 2.90Å) and **24** (blue) (PDB code: 4N3R, resolution: 1.90 Å) [34].

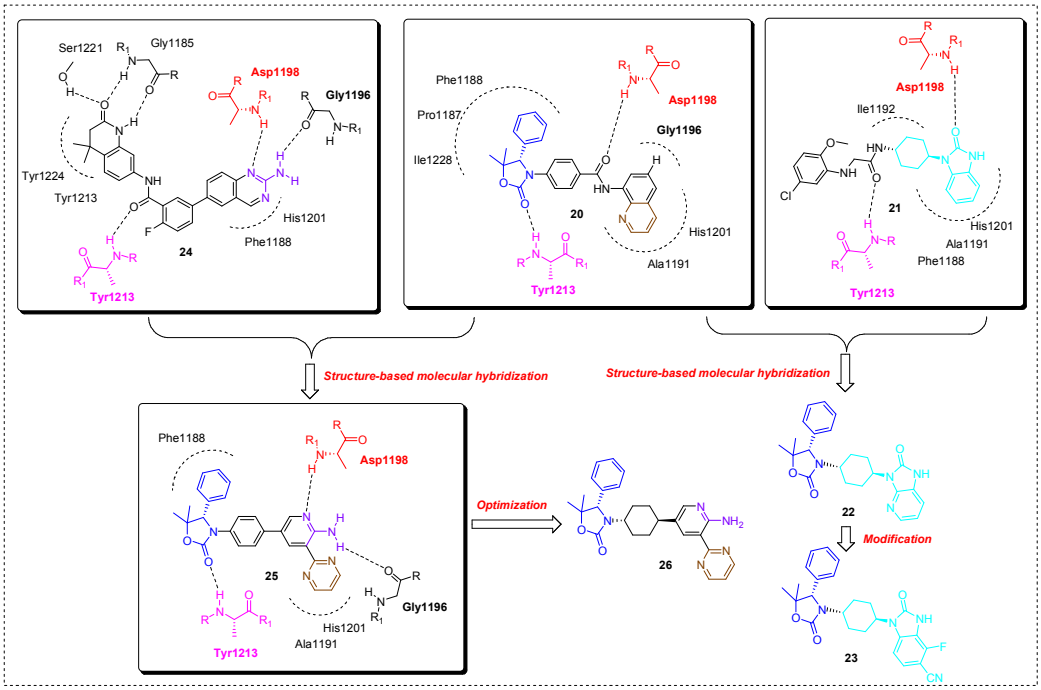

Figure 20. Chemdraw representation of crystallographic overlays-based molecular hybridization. Herein, the rationale behind this concept was summarized and case studies were presented.

Compound **24** was identified as a novel and potent TNKSI *via* HTS approach (TNKS, IC_{50} = 0.15 μM; TBC, IC_{50} = 2.0 μM; PARP1, IC_{50} > 85 μM). A co-crystal structure of TNKS1/**24** complex revealed that **24** occupied both the conserved nicotinamide pocket and the induced pocket simultaneously, similar to that of other recently reported TNKSIs with dual-binding mode. The dihydroquinolinone group resided in the nicotinamide pocket with the C=O group engaging in a H-bond interaction with Ser1221 and the nitrogen H-bond to Gly1185. The aminoquinazoline moiety occupied the induced pocket, with the amino group hydrogen bonded to Gly1196, and N1 hydrogen bonded to Asp1198 (**Figure 19**) [34]. An overlay of the co-crystal structures of **20** and **24** complexed with TNKS1 inspired a hypothesis that replacing the labile aminoquinazoline amide of **24** with other counterparts would enhance plasma metabolic stability while keeping two important H-bond interactions with the target (**Figure 20**).

It was envisioned that the aminopyridine group would serve as a simplified mimic of

the aminoquinazoline moiety in **24**. Positioning a pyrimidinyl ring in the 3-positon would engage the critical π-stacking interaction with His1201, as seen with the quinoline group in **20**. It's gratifying that, compound **25** demonstrated high TNKS inhibitory effect while showing favorable selectivity *versus* PARP1/2. Compound **25** could promote accumulation of Axin (EC_{50} = 0.709 μM), and suppress β-catenin accumulation (TBC IC_{50} = 0.233 μM) and Wnt reporter gene transcription (STF IC_{50} = 0.096 μM) in cellular assays. What is more, it was stable in rat and human liver microsomes (RLM/HLM Clint = 48/33 μL/min/mg), and shown to be suitable for further investigation.

Furthermore, the activity was dramatically increased by replacing the central phenyl group of **25** with a saturated cyclohexyl moiety. The stereochemistry of the cyclohexyl moiety impacted the potency greatly. For instance, the trans-isomer **26** (TNKS1/2, IC_{50} = 2 nM) displayed significantly increased enzymatic and cellular potency over **25**, while the cis-isomer was less active [34]. The binding mode of all bioactive compounds was investigated by X-ray crystallography (**Figures 21-23**), which allowed to explain their potency and selectivity and to establish a structural basis for rational optimization towards highly active and selective TNKSIs.

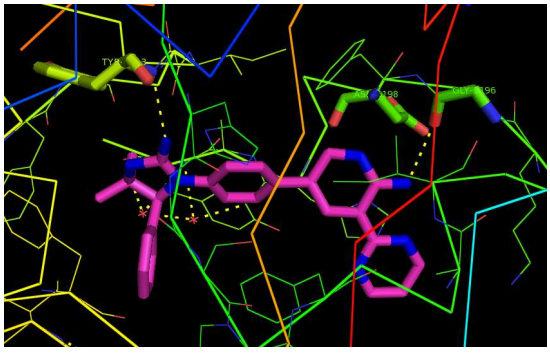

Figure 21. Co-crystal structure of TNKS1 with compound **25** (carbon: pink) (PDB code: 4N4T, resolution: 2.32Å).

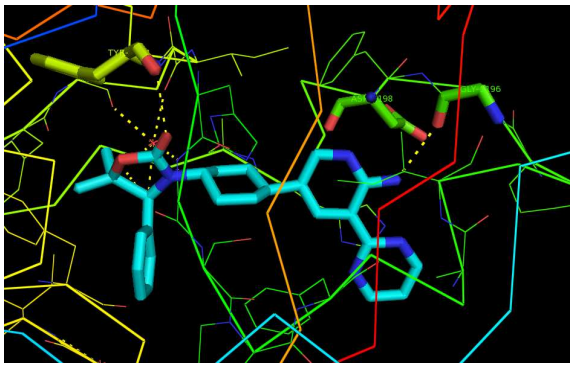

Figure 22. Co-crystal structure of TNKS1 with **26** (carbon: blue) (PDB code: 4N4V, resolution: 2.00Å).

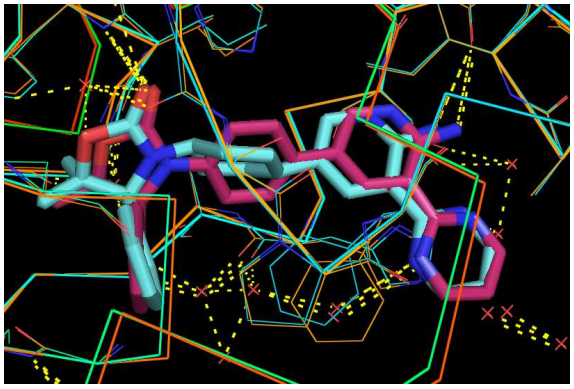

Figure 23. Overlay of the TNKS1 co-crystal structure of **25** (carbon: pink) (PDB code: 4N4T) and **26** (blue) (PDB code: 4N4V).

3.4 Structure- and biophysics-driven fragment-based ligand design (FBLD) strategy

Fragment-based drug discovery (FBDD) is an effective paradigm in drug discovery that affords more efficiently bioactive lead compounds as well as original structural scaffolds by utilizing very compact fragments [35].

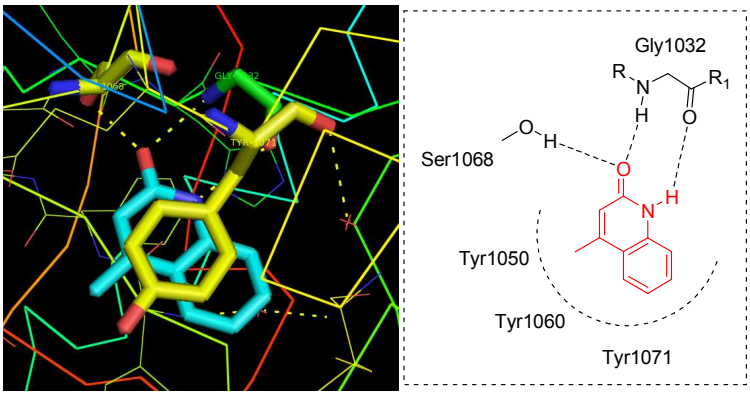

Figure 24. Co-crystal structure of TNKS2 with compound **27** (carbon: blue) (PDB code: 3W51, resolution: 2.00 Å).

4-Methyl-1,2-dihydroquinolin-2-one (**27**) was identified as a highly potent fragment binding in the nicotinamide-binding pocket using a thermal shift assay-based biophysical screening. Then, guided by co-crystal structures of TNKS/TNKSI complex (**Figure 24**), evolution of this compound in the first turn of expansion along its 7-position resulted in dramatic potency improvements (**Figure 25**). Most notably, 2-fluorophenyl substituted derivative **28** displayed more than 16-fold selectivity for TNKS2 *versus* TNKS1 (**Table 3**). Generally, TNKS inhibition has been investigated as concurrent inhibition of TNKS1/2, and the detailed information of the specific contribution from the two isoforms is ill-defined. Therefore, these novel TNKS2-selective molecules could afford a valuable pharmacological tool to investigate the implications of each TNKS isoforms in physiopathological conditions. A crystal structure of **28** (**Figure 26**) demonstrated that the nonplanar molecule extended with its fluorine atom into a subpocket, which coincided with a region of the active site where structural dissimilarities were observed between TNKSs and other members in PARP family. A new cycle of optimization generated derivatives (such as **29**) with high affinities (IC_{50} values in the low nanomolar level), favorable selectivity, ligand efficiency, and good solubility [36]. Co-crystal structure of TNKS2 with **29** (**Figure 27**) revealed the binding orientation of these molecules and provided critical insights for further optimizations of back-up derivatives towards improving their potency while maintaining their selectivity profiles.

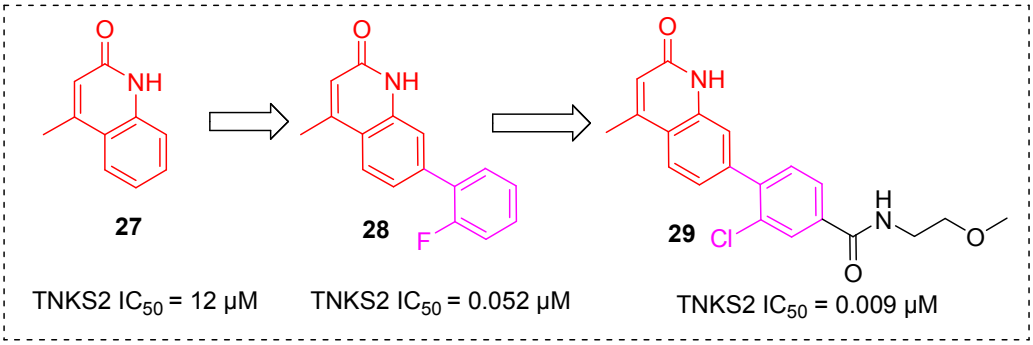

Figure 25. Chemdraw representation of structure- and biophysics-driven FBLD strategy converting fragment **27** into leads **28** and **29**.

Table 3. IC_{50} (μM) and PARP selectivity of XAV939 and **28**.

Compd	PARP1	PARP2	PARP3	TNKS1	TNKS2	PARP6
28	>10	>10	>10	0.86	0.052	>10
XAV939	0.12	0.046	>10	0.011	0.088	>10

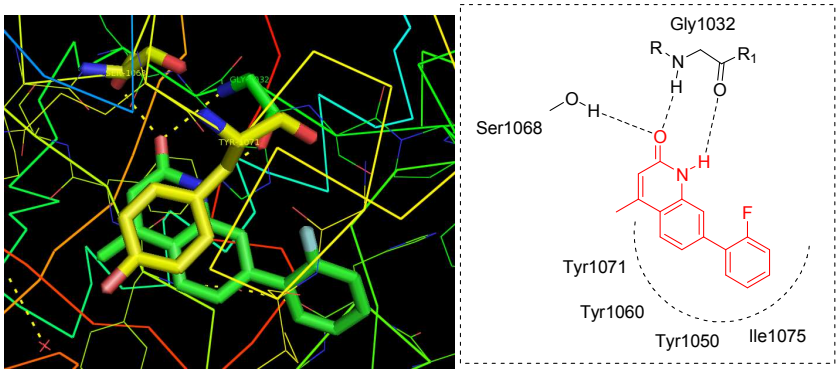

Figure 26. Co-crystal structure of TNKS2 with **28** (carbon: green) (PDB code: 4IUE, resolution: 2.38Å).

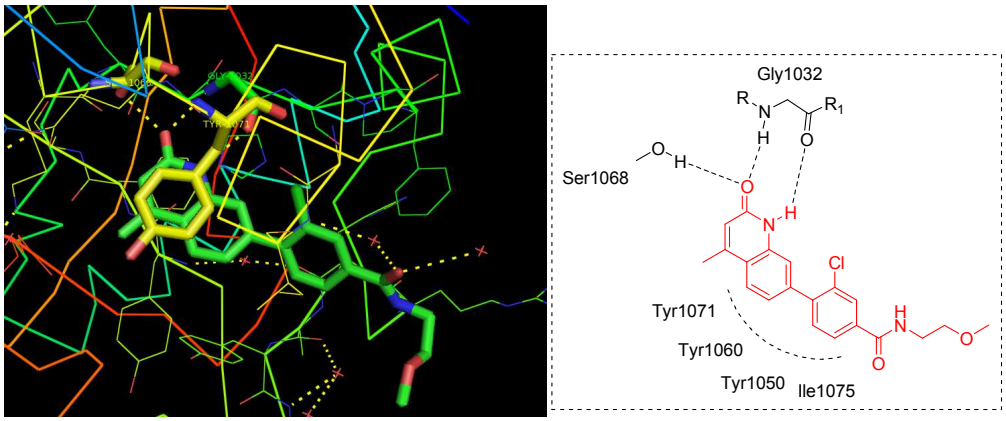

Figure 27. Co-crystal structure of TNKS2 with **29** (carbon: green) (PDB code: 4J3L, resolution: 2.09Å).

3.5 Structure-based bioisosteric replacement

It is well-known in medicinal chemistry that the bioisosteric refinement of the central core in bioactive compounds combined with introducing privileged substituents is an excellent tool and common practice for lead optimization to find proprietary and novel back-up analogues with desired potency, selectivity and the required ADME profiles [37].

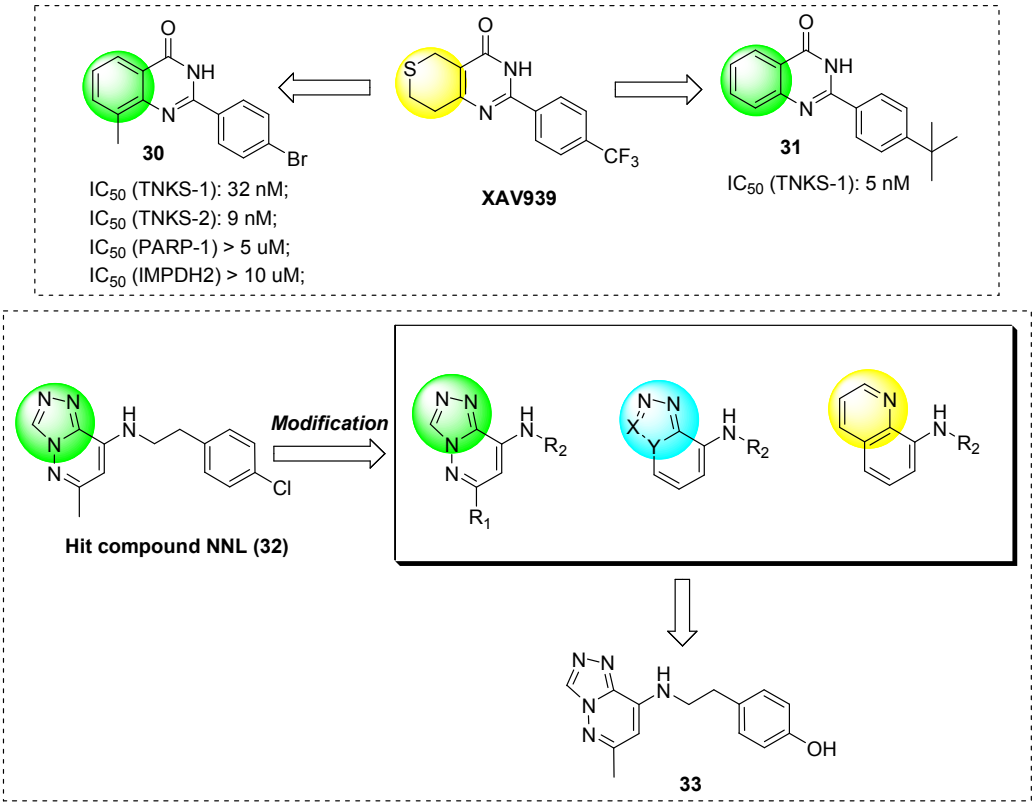

Figure 28. Chemdraw representation of bioisosteric replacement in the discovery of novel TNKSIs.

In searching for selective TNKSIs, a group of 2-arylquinazolin-4-ones were designed and identified as efficient and selective TNKSIs *via* bioisosteric replacement (**Figure 28**), some being more active and selective than the lead compound XAV939, with IC_{50} = 3 nM against TNKS-2 (compound **30**). Structural elements important for interactions with the target were established, for instance, methyl at the 8-position seems to be optimum for inhibition and various substituents were tolerated at the *para*-position of the 2-phenyl group. These compounds were highly selective for inhibition of TNKS1/2, showing much weaker activity against PARPs and no effect on IMPDH2 (an NAD^+-requiring oxidoreductase) [38].

In addition, a series of 2-phenyl-3,4-dihydroquinazolin-4-one derivatives was identified as highly potent TNKSIs. Substitutions at the *para*-position of the phenyl group were confirmed as a valuable venue for increasing potency and improving selectivity. The best compound **31** displayed strong potencies in single-digit nanomolar level (TNKS1, IC_{50} = 5 nM), and it did not inhibit the other PARPs

members at a concentration up to 10 mM. The activity of **31** was equally as strong as that of XAV939 (TNKS1, IC_{50} = 11 nM). Gratifyingly, **31** was more selective than XAV939. It also demonstrated very potent inhibition of Wnt signaling and antagonism of the Wnt pathway with comparable activity with IWR-1. Collectively, **31** was an excellent molecular probe to inhibit TNKSs selectively and explore the influences of cell-active TNKSs inhibition [39].

6,8-Disubstituted triazolo[4,3-b]piridazine (NNL, **32**) was characterized biologically as one starting hit compound of TNKSI. Although the amide feature was lost in NNL (**32**), all the interactions formed by the canonical PARP inhibitors that bind in the traditional site, were still existed (**Figure 29**) [40]. In order to define structure-activity relationships (SARs) around this unexplored scaffold, structure-based optimization of NNL (**32**) *via* bioisosteric refinement of the central core combined with introducing diverse substituents was performed, which led to the discovery of TNKSI **33**, endowed with low nanomolar values of IC_{50} on TNKSs and was devoided of activity towards any other PARPs isoforms (**Table 4**). As ascertained by crystallographic analysis, it worked as NAD isostere (**Figure 30**) [41]. This research formed a solid basis for rational development of triazolo[4,3-b]piridazines as TNKSIs and guides the modifications of other structurally related compounds.

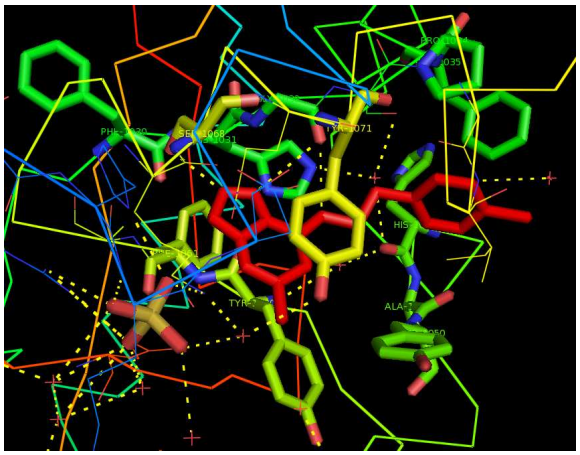

Figure 29. Co-crystal structure of catalytic PARP domain of TNKS2 with **32** (PDB code: 3P0Q, resolution: 1.90Å).

Table 4. IC_{50} (μM) and PARP selectivity of XAV939 and **33**.

Compd	PARP1	PARP2	PARP3	TNKS1	TNKS2	PARP6

33	>10	>10		0.012	0.2	
XAV939	0.12	0.046	>10	0.011	0.088	>10

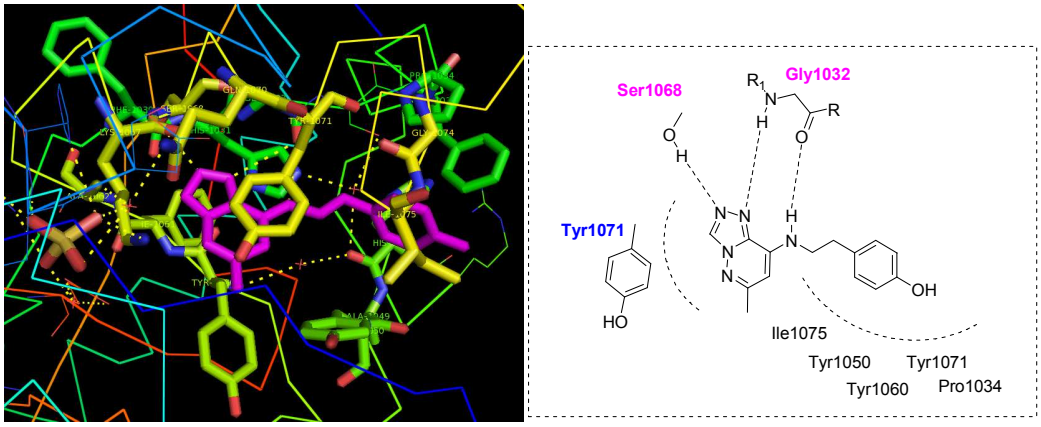

Figure 30. Co-crystal structure of catalytic PARP domain of TNKS2 with **33**. (PDB code: 4M7B, resolution: 1.95Å).

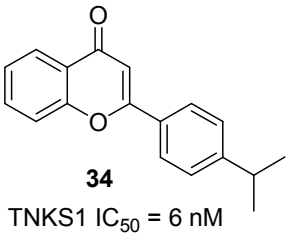

34

TNKS1 IC_{50} = 6 nM

What not allow to ignore is, for newly emerging drug targets, the establishment of efficient assay systems is of crucial importance. Now the efficient assay systems for TNKSIs screening, including the yeast cell-based screen [42] and homogeneous screening assay [43,44] have been established, which allow rapid identification of inhibitory activity against TNKSs and are amenable to HTS using robotics. A validatory screen with a natural product and synthesized analogues library confirmed suitability of the assay for seeking novel TNKSIs. Flavone MN-64 (**34**), displayed 6 nM potency against TNKS1, favorable isoenzyme selectivity, and Wnt signaling inhibition [45]. Future efforts should focus on further improvement of selectivity profiles as the flavones have demonstrated biological activities toward a broad range of medicinal targets.

4. Conclusions and prospects

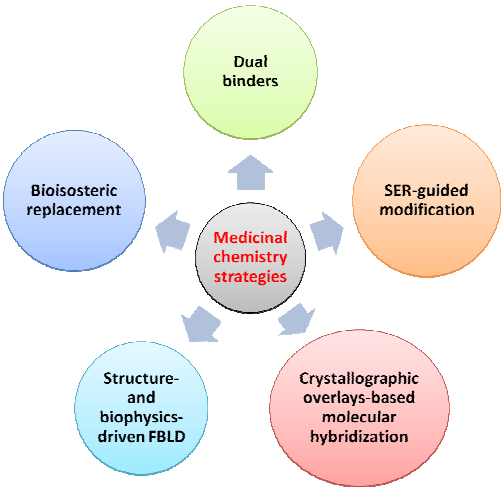

Figure 31. Medicinal chemistry strategies employed in the discovery of TNKSIs.

Our goal in producing this review is to afford critical insights for the most important strategies used in discovery of TNKSIs *via* structure-based drug design (**Figure 31**). Beyond this, we aim to illustrate how these strategies are being applied in current efforts towards discovery of potent and isoform-selective TNKSIs.

Obviously, several families of TNKSIs have been described in recent literatures; however, up to now, none of them have generated a clinical candidate. It is certain that the selectivity profile is an important aspect in elucidating the function of individual TNKS enzymes in the development of next generation TNKSIs as therapeutic agents . Undoubtedly, understanding the detailed structural information about specific TNKS/TNKSI interactions, chemical space around the binding pocket and overall shape with energetically accessible geometries should lead to more sophisticated, evidenced-based development of next generation TNKSIs with increased potency and improved selectivity profiles. Though structure-based rational design approaches have been discussed separately in this review, no method has proven to be a "one size fits all" route, it is clear that only multidisciplinary coordination could better help to facilitate lead optimization. Besides, several other approaches including diversity-oriented synthesis (DOS), dynamic combinatorial chemistry (DCC), and in situ click chemistry in combination with HTS technologies (such as microarrays) display complementary features and can be strategically used to explore biologically-relevant chemical space of TNKSs and to further revolutionize the lead discovery and optimization steps in drug research.

Acknowledgment

The financial support from the National Natural Science Foundation of China (NSFC No.81102320, No.81273354), Research Fund for the Doctoral Program of Higher Education of China (No.20110131130005, 20110131120037), and China Postdoctoral Science Foundation funded project (No.20100481282, 2012T50584) is gratefully acknowledged.

All the figures of binding modes were generated using PyMol (www.pymol.org).

The authors declare no conflict of interest.

References

[1] (a) J. L. Riffell, C. J. Lord, and A. Ashworth, Tankyrase-targeted therapeutics: expanding opportunities in the PARP family, *Nat. Rev. Drug Discov.*, 2012, **11**, 923-936. (b) S. Vyas, and P. Chang, New PARP targets for cancer therapy, Nat. Rev. Cancer, 2014, **14**, 502-509.

[2] V. Schreiber, F. Dantzer, J. C. Ame, and G. de Murcia, Poly(ADP-ribose): novel functions for an old molecule, *Nat. Rev. Mol. Cell Biol.,* 2006, **7**, 517-528.

[3] A. M. Busch, K. C. Johnson, R. V. Stan, A. Sanglikar, Y, Ahmed, E. Dmitrovsky, and S. J. Freemantle, Evidence for tankyrases as antineoplastic targets in lung cancer, *BMC Cancer,* 2013, **13**, 211.

[4] L. Lehtiö, N. W. Chi, and S. Krauss, Tankyrases as drug targets, *FEBS J.,* 2013, **280**, 3576-3593.

[5] P. Liscio, E. Camaioni, A. Carotti, R. Pellicciari, and A. Macchiarulo, From polypharmacology to target specificity: the case of PARP inhibitors, *Curr. Top Med. Chem.,* 2013, **13**, 2939-2954.

[6] (a) B. Chen, M. E. Dodge, W. Tang, J. Lu, Z. Ma, C. W. Fan, S. Wei, W. Hao, J. Kilgore, N. S. Williams, M. G. Roth, J. F. Amatruda, C. Chen, and L. Lum, Small molecule-mediated disruption of Wnt-dependent signaling in tissue regeneration and cancer, *Nat. Chem. Biol.*, 2009, **5**, 100-107; (b) J. Lu, Z. Ma, J. C. Hsieh, C. W. Fan, B. Chen, J. C. Longgood, N. S. Williams, J. F. Amatruda, L. Lum, and C. Chen, Structure-activity relationship studies of small-molecule inhibitors of Wnt response, *Bioorg. Med. Chem. Lett.,* 2009, **19**, 3825-3827.

[7] S. M. Huang, Y. M. Mishina, S. Liu, A. Cheung, F, Stegmeier, G. A. Michaud, O. Charlat, E. Wiellette, Y. Zhang, S. Wiessner, M. Hild, X. Shi, C. J. Wilson, C. Mickanin, V. Myer, A.

Fazal, R. Tomlinson, F. Serluca, W. Shao, H. Cheng, M. Shultz, C. Rau, M. Schirle, J. Schlegl, S. Ghidelli, S. Fawell, C. Lu, D. Curtis, M. W. Kirschner, C. Lengauer, P. M. Finan, J. A. Tallarico, T. Bouwmeester, J. A. Porter, A. Bauer, and F. Cong, Tankyrase inhibition stabilizes axin and antagonizes Wnt signalling, *Nature,* 2009, **461**, 614-620.

[8] E.R. Fearon, PARsing the phrase "all in for Axin"- Wnt pathway targets in cancer, *Cancer Cell,* 2009, **16**, 366-368.

[9] C. Liu, and X. He, Destruction of a destructor: a new avenue for cancer therapeutics targeting the Wnt pathway, *J. Mol. Cell Biol.,* 2010, **2**, 70-73.

[10] X. H. Tian, W. J. Hou, Y. Fang, J. Fan, H. Tong, S. L. Bai, Q. Chen, H. Xu, and Y. Li, XAV939, a tankyrase 1 inhibitior, promotes cell apoptosis in neuroblastoma cell lines by inhibiting Wnt/β-catenin signaling pathway, *J. Exp. Clin. Cancer Res.*, 2013, **32**, 100.

[11] (a) J. Waaler, O. Machon, J. P. von Kries, S. R. Wilson, E. Lundenes, D. Wedlich, D. Gradl, J. E. Paulsen, O. Machonova, J. L. Dembinski, H. Dinh, and S. Krauss, Novel synthetic antagonists of canonical Wnt signaling inhibit colorectal cancer cell growth, *Cancer Res.,* 2011, 71, 197-205. (b) E. Wessel Stratford, J. Daffinrud, E. Munthe, R. Castro, J. Waaler, S. Krauss, and O. Myklebost, The tankyrase-specific inhibitor JW74 affects cell cycle progression and induces apoptosis and differentiation in osteosarcoma cell lines, *Cancer Med.*, 2014, **3**, 36-46.

[12] M. D. Shultz, C. A. Kirby, T. Stams, D. N. Chin, J. Blank, O. Charlat, H. Cheng, A. Cheung, F. Cong, Y. Feng, P. D. Fortin, T. Hood, V. Tyagi, M. Xu, B. Zhang, and W. Shao, [1,2,4]triazol-3-ylsulfanylmethyl)-3-phenyl-[1,2,4]oxadiazoles: antagonists of the Wnt pathway that inhibit tankyrases 1 and 2 via novel adenosine pocket binding, *J. Med. Chem.*, 2012, **55**, 1127-1136.

[13] A. Voronkov, D. D. Holsworth, J. Waaler, S. R. Wilson, B. Ekblad, H. Perdreau-Dahl, H. Dinh, G. Drewes, C. Hopf, J. P. Morth, and S. Krauss, Structural basis and SAR for G007-LK, a lead stage 1,2,4-triazole based specific tankyrase 1/2 inhibitor, *J. Med. Chem.,* 2013, **56**, 3012-3023.

[14] T. Lau, E. Chan, M. Callow, J. Waaler, J. Boggs, R. A. Blake, S. Magnuson, A. Sambrone, M. Schutten, R. Firestein, O. Machon, V. Korinek, E. Choo, D. Diaz, M. Merchant, P. Polakis, D. D. Holsworth, S. Krauss, and M. Costa, A novel tankyrase small-molecule inhibitor suppresses APC mutation-driven colorectal tumor growth, *Cancer Res.,* 2013, **73**, 3132-3144.

[15] R. G. James, K. C. Davidson, K. A. Bosch, T. L. Biechele, N. C. Robin, R. J. Taylor, M. B. Major, N. D. Camp, K. Fowler, T. J. Martins, and R. T. Moon, WIKI4, a novel inhibitor of tankyrase and Wnt/ß-catenin signaling, *PLoS. One,* 2012, **7,** e50457.

[16] T. Haikarainen, H. Venkannagari, M. Narwal, E. Obaji, H. W. Lee, Y. Nkizinkiko, and L. Lehtiö, Structural basis and selectivity of tankyrase inhibition by a Wnt signaling inhibitor WIKI4, *PLoS. One,* 2013, **8**, e65404.

[17] J. Waaler, O. Machon, L. Tumova, H. Dinh, V. Korinek, S. R. Wilson, J. E. Paulsen, N. M. Pedersen, T. J. Eide, O. Machonova, D. Gradl, A. Voronkov, J. P. von Kries, and S. Krauss, A novel tankyrase inhibitor decreases canonical Wnt signaling in colon carcinoma cells and reduces tumor growth in conditional APC mutant mice, *Cancer Res.,* 2012, **72**, 2822-2832.

[18] T. Karlberg, N. Markova, I. Johansson, M. Hammarström, P. Schütz, J. Weigelt, and H. Schüler, Structural basis for the interaction between tankyrase-2 and a potent Wnt-signaling inhibitor, *J. Med. Chem.,* 2010, **53**, 5352-5355.

[19] C. A. Kirby, A. Cheung, A. Fazal, M. D. Shultz, and T. Stams, Structure of human tankyrase 1 in complex with small-molecule inhibitors PJ34 and XAV939, *Acta. Crystallogr. Sect. F. Struct. Biol. Cryst. Commun.,* 2012, **68**, 115-118.

[20] H. Gunaydin, Y. Gu, and X. Huang, Novel binding mode of a potent and selective tankyrase inhibitor, *PLoS. One,* 2012, **7**, e33740.

[21] M. Narwal, H. Venkannagari, and L. Lehtiö, Structural basis of selective inhibition of human tankyrases, *J. Med. Chem.,* 2012, **55**, 1360-1367.

[22] T. Haikarainen, M. Narwal, P. Joensuu, and L. Lehtiö, Evaluation and Structural Basis for the Inhibition of Tankyrases by PARP Inhibitors, *ACS. Med. Chem. Lett.*, 2013, **5**, 18-22.

[23] Y. Song, P. Zhan, X. Li, D. Rai, E. De Clercq, and X. Liu, Multivalent agents: a novel concept and preliminary practice in Anti-HIV drug discovery, *Curr. Med. Chem.,* 2013, **20**, 815-832.

[24] H. Bregman, H. Gunaydin, Y. Gu, S. Schneider, C. Wilson, E. F. DiMauro, and X. Huang, Discovery of a class of novel tankyrase inhibitors that bind to both the nicotinamide pocket and the induced pocket, *J. Med. Chem.,* 2013, **56**, 1341-1345.

[25] Z. Hua, H. Bregman, J. L. Buchanan, N. Chakka, A. Guzman-Perez, H. Gunaydin, X. Huang, Y. Gu, V. Berry, J. Liu, Y. Teffera, L. Huang, B. Egge, R. Emkey, E. L. Mullady, S. Schneider, P.

S. Andrews, L. Acquaviva, J. Dovey, A. Mishra, J. Newcomb, D. Saffran, R. Serafino, C. A. Strathdee, S. M. Turci, M. Stanton, C. Wilson, and E. F. Dimauro, Development of novel dual binders as potent, selective, and orally bioavailable tankyrase inhibitors, *J. Med. Chem.,* 2013, **56**, 10003-10015.

[26] (a) A. L. Hopkins, C. R. Groom, and A. Alex, Ligand efficiency: a useful metric for lead selection, Drug Discov. Today, 2004, 9, 430-431; (b) C. Abad-Zapatero, and J. T. Metz, Ligand efficiency indices as guideposts for drug discovery, *Drug Discov. Today,* 2005, **10**, 464-469.

[27] C. W. Murray, D. A. Erlanson, A. L. Hopkins, G. M. Keserü, P. D. Leeson, D. C. Rees, C. H. Reynolds, and N. J. Richmond, Validity of ligand efficiency metrics, *ACS. Med. Chem. Lett.*, 2014, **5**, 616-618.

[28] P. D. Leeson, and B. Springthorpe, The influence of drug-like concepts on decision making in medicinal chemistry, *Nat. Rev. Drug Discov.,* 2007, **6**, 881-890.

[29] M. D. Shultz, A. K. Cheung, C. A. Kirby, B. Firestone, J. Fan, Z. Chen, D. N. Chin, L. Dipietro, A. Fazal, Y. Feng, P. D. Fortin, T. Gould, B. Lagu, H. Lei, F. Lenoir, D. Majumdar, E. Ochala, M. G. Palermo, L. Pham, M. Pu, T. Smith, T. Stams, R. Tomlinson, B. B. Touré, M. Visser, R. Wang, N. J. Waters, and W. Shao, Identification of NVP-TNKS656 - the use of structure efficiency relationships to generate a highly potent, selective and orally active tankyrase inhibitor, *J. Med. Chem.,* 2013, **56**, 6495-6511.

[30] M. D. Shultz, D. Majumdar, D. N. Chin, P. D. Fortin, Y. Feng, T. Gould, C. A. Kirby, T. Stams, N. J. Waters, and W. Shao, Structure efficiency relationship of [1,2,4]triazol-3-ylamines as novel nicotinamide isosteres that inhibit tankyrases, *J. Med. Chem.,* 2013, **56**, 7049-7059.

[31] C. Viegas-Junior, A. Danuello, V. da Silva Bolzani, E. J. Barreiro, and C. A. Fraga, Molecular hybridization: a useful tool in the design of new drug prototypes, *Curr. Med. Chem.,* 2007, **14**, 1829-1852.

[32] L. H. Jones, G. Allan, O. Barba, C. Burt, R. Corbau, T. Dupont, T. Knöchel, S. Irving, D. S. Middleton, C. E. Mowbray, M. Perros, H. Ringrose, N. A. Swain, R. Webster, M. Westby, and C. Phillips, Novel indazole non-nucleoside reverse transcriptase inhibitors using molecular hybridization based on crystallographic overlays, *J. Med. Chem.,* 2009, **52**, 1219-1223.

[33] H. Bregman, N. Chakka, A. Guzman-Perez, H. Gunaydin, Y. Gu, X. Huang, V. Berry, J. Liu, Y. Teffera, L. Huang, B. Egge, E. L. Mullady, S. Schneider, P. S. Andrews, A. Mishra, J.

Newcomb, R. Serafino, C. A. Strathdee, S. M. Turci, C. Wilson, and E. F. DiMauro, Discovery of novel, induced-pocket binding oxazolidinones as potent, selective, and orally bioavailable tankyrase inhibitors, *J. Med. Chem.,* 2013, **56**, 4320-4342.

[34] H. Huang, A. Guzman-Perez, L. Acquaviva, V. Berry, H. Bregman, J. Dovey, H. Gunaydin, X. Huang, L. Huang, D. Saffran, R. Serafino, S. Schneider, C. Wilson, and E. F. DiMauro, Structure-based design of 2-aminopyridine oxazolidinones as potent and selective tankyrase inhibitors. *ACS. Med. Chem. Lett.,* 2013, **4**, 1218-1223.

[35] M. J. Hartshorn, C. W. Murray, A. Cleasby, M. Frederickson, I. J. Tickle, and H. Jhoti, Fragment-based lead discovery using X-ray crystallography, *J. Med. Chem.,* 2005, **48**, 403-413.

[36] E. A. Larsson, A. Jansson, F. M. Ng, S. W. Then, R. Panicker, B. Liu, K. Sangthongpitag, V. Pendharkar, S. J. Tai, J. Hill, C. Dan, S. Y. Ho, W. W. Cheong, A. Poulsen, S. Blanchard, G. R. Lin, J. Alam, T. H. Keller, and P. Nordlund, Fragment-based ligand design of novel potent inhibitors of tankyrases, *J. Med. Chem.,* 2013, **56**, 4497-4508.

[37] G. A. Patani, and E. J. LaVoie, Bioisosterism: A Rational Approach in Drug Design. *Chem. Rev.*, 1996, **96**, 3147-3176.

[38] A. Nathubhai, P. J. Wood, M. D. Lloyd, A. S. Thompson, and M. D. Threadgill, Design and Discovery of 2-arylquinazolin-4-ones as potent and selective inhibitors of tankyrases, *ACS. Med. Chem. Lett.,* 2013, **4**, 1173-1177.

[39] T. Haikarainen, J. Koivunen, M. Narwal, H. Venkannagari, E. Obaji, P. Joensuu, T. Pihlajaniemi, and L. Lehtiö, para-Substituted 2-phenyl-3,4-dihydroquinazolin-4-ones as potent and selective tankyrase inhibitors, *ChemMedChem,* 2013, **8**, 1978-1985.

[40] E. Wahlberg, T. Karlberg, E. Kouznetsova, N. Markova, A. Macchiarulo, A. G. Thorsell, E. Pol, A. Frostell, T. Ekblad, D. Oncü, B. Kull, G. M. Robertson, R. Pellicciari, H. Schüler, and J. Weigelt, Family-wide chemical profiling and structural analysis of PARP and tankyrase inhibitors, *Nat. Biotechnol.*, 2012, **30**, 283-288.

[41] P. Liscio, A. Carotti, S. Asciutti, T. Karlberg, D. Bellocchi, L. Llacuna, A. Macchiarulo, S. A. Aaronson, H. Schüler, R. Pellicciari, and E. Camaioni, Design, synthesis, crystallographic studies, and preliminary biological appraisal of new substituted

triazolo[4,3-b]pyridazin-8-amine derivatives as tankyrase inhibitors, *J. Med. Chem.,* 2014, **57**, 2807-2812.

[42] Y. Yashiroda, R. Okamoto, K. Hatsugai, Y. Takemoto, N. Goshima, T. Saito, M. Hamamoto, Y. Sugimoto, H. Osada, H. Seimiya, and M. Yoshida, A novel yeast cell-based screen identifies flavone as a tankyrase inhibitor, *Biochem. Biophys. Res. Commun.*, 2010, **394**, 569-573.

[43] M. Narwal, A. Fallarero, P. Vuorela, and L. Lehtiö, Homogeneous screening assay for human tankyrase, *J. Biomol. Screen,* 2012, **17**, 593-604.

[44] M. Narwal, T. Haikarainen, A. Fallarero, P. M. Vuorela, and L. Lehtiö, Screening and structural analysis of flavones inhibiting tankyrases, *J. Med. Chem.*, 2013, **56**, 3507-3517.

[45] M. Narwal, J. Koivunen, T. Haikarainen, E. Obaji, O. E. Legala, H. Venkannagari, P. Joensuu, T. Pihlajaniemi, and L. Lehtiö, Discovery of tankyrase inhibiting flavones with increased potency and isoenzyme selectivity, *J. Med. Chem.,* 2013, **56**, 7880-7889.

Biographies

Dr. Peng Zhan was born in 1983 in Ji'nan, Shandong province, China. He obtained his B.S. degree from Shandong University, China, in 2005. Then he earned his M.S. degree and Ph.D in medicinal chemistry from Shandong University under the guidance of Prof. Xinyong Liu in 2008 and 2010, respectively. In 2012, he was appointed as a JSPS (Japan Society for the Promotion of Science) Postdoctoral Fellow in Graduate School of Medical Science, Kyoto Prefectural University of Medicine, Japan under the guidance of Professor Takayoshi Suzuki. He is now working as an associate professor

in Shandong University. So far he has published more than 50 SCI academic peer review papers.

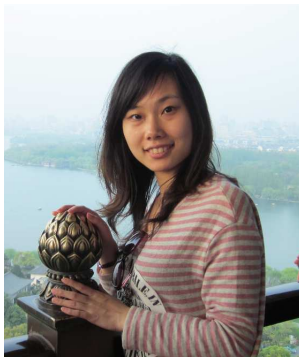

Yu'ning Song was born in 1984 in Jinan, Shandong province, China. In 2007, she graduated from China pharmaceutical university. Then in 2010, she earned her master degree in pharmacology from Shandong University. She is currently studying for Ph.D degree in the School of Pharmaceutical Science in Shandong University.

Yukihiro Itoh obtained his Ph.D in pharmaceutical sciences from the University of Tokyo (2011). Subsequently, he worked as a research associate at the Scripps Reasearch Institute (2011-2012). During that time, he was a Research Fellow of the Japan Society for the Promotion of Science (2010-2012). He is currently an Assistant Professor at the Graduate School of Medical Science, Kyoto Prefectural University of Medicine, Japan (2012 to present). His research interests are focused on medicinal chemistry and chemical biology, including synthesis of bioactive small molecules, analysis of the mechanisms of their interaction with biological targets, and mechanisms of pharmacological action.

Takayoshi Suzuki received his B.Sc. and M.Sc. from the University of Tokyo (1995 and 1997, respectively), then became a Researcher at Japan Tobacco Inc. (1997–2002). He subsequently joined the Graduate School of Pharmaceutical Sciences, Nagoya City University, as an Assistant Professor (2003–2009) and Lecturer (2009–2011). During that time, he received his Ph.D. from the Graduate School of Pharmaceutical Sciences, the University of Tokyo. He is currently a full Professor at the Graduate School of Medical Science, Kyoto Prefectural University of Medicine (2011 to present). His research interests are in the areas of medicinal chemistry and bioorganic chemistry.

Prof. Dr. Xinyong Liu was born in 1963 in Qingdao, Shandong province, China. He received his B.S. and M.S. degrees from School of Pharmaceutical Sciences, Shandong University, in 1984 and in 1991, respectively. From 1997 to 1999 he worked at Instituto de Quimica Medica (CSIC) in Spain as a senior visiting scholar. He obtained his Ph.D. from Shandong University in 2004. He is currently the Director

of the Institute of Medicinal Chemistry, Shandong University. His research area involves discovery of bioactive molecules based on rational drug design approaches. He has contributed to more than 200 scientific publications and patents as well as many monographs.

2014-08-16